A sweet new set of inducible and constitutive promoters for haloarchaea

Theopi Rados[1†], Katherine Andre[1†], Micaela Cerletti[1,2]*, and Alex Bisson[1]*

[1] Brandeis University, Department of Biology, Waltham, MA 02453, USA
[2] Instituto de Investigaciones Biológicas, Facultad de Ciencias Exactas y Naturales, Universidad Nacional de Mar del Plata, Mar del Plata, Argentina

[†] These authors contributed equally to this work and share the first authorship
* Co-corresponding authors.
Correspondence should be addressed to bisson@brandeis.edu

Inducible promoters are one of the most important technical tools for cellular and molecular biology. The ability to deplete, replete, and overexpress genes on demand is the foundation of most functional studies. Here, we develop and characterize a new xylose-responsive promoter (Pxyl), the second inducible promoter system for the model haloarcheon *Haloferax volcanii*. Generating RNA-seq datasets from cultures in the presence of four historically used inducers (arabinose, xylose, maltose, and IPTG), we mapped upregulated genomic regions largely repressed in the absence of the above inducers. The most upregulated promoter was found to control the expression of the *xacEA* (*HVO_B0027-28*) operon in the pHV3 chromosome. To characterize this promoter region, we cloned msfGFP (monomeric superfold green fluorescent protein) under the control of two different 5' UTR fragments into a modified pTA962 vector: the first 250 bp (P250) and the whole 750 bp intergenic region (P750). The P250 region showed to express msfGFP constitutively and its expression does not respond to the presence or absence of xylose. However, the P750 promoter showed not only to be repressed in the absence of xylose but also expressed higher levels of msfGFP in the presence of the inducer. Finally, we validated our new inducible Pxyl promoter by reproducing morphological phenotypes already described in the literature. By overexpressing the tubulin-like FtsZ1 or FtsZ2, we observed similar, but slightly more pronounced morphological defects compared to the tryptophan-inducible promoter PtnaA. FtsZ1 overexpression created larger, deformed cells, whereas cells overexpressing FtsZ2 were smaller but mostly retained their shape. In summary, this work contributes with a new xylose-inducible promoter Pxyl that can be used simultaneously with the well-established PtnaA in functional studies in *H. volcanii*.

Introduction

Inducible promoters have been essential tools for molecular and cell biology studies in bacteria and eukaryotes, allowing both temporal and expression control of the expression of genes of interest. Among the multiple uses of inducible promoters are dynamic studies of gene expression *in vivo*, timed expression of tagged protein fusions, and depletion assays of essential genes. On the other hand, constitutive promoters have a wide range of applications from expressing selective marker genes to consistent overexpression of proteins.

Like most model organisms, the budding yeast *Saccharomyces cerevisiae* has a breadth of inducible promoters, most relying on ethanol and sugars (Weinhandl et al., 2014). In animal cells, the inducible promoters available range from the endogenous hormone and stress-responsive promoters, which have later been replaced by variations of bacterial promoters due to tighter control of the latter. Mammalian cells can also be studied with two options of light-induced promoters, based on a light-oxygen-voltage (LOV) domain from the fungus *Neurospora crassa* and on the *Arabidopsis* photoreceptor (Kallunki et al., 2019), which have been used in the research and identification of important signaling pathways such as mTOR and Hippo (Kallunki et al., 2019). In plants, there is also a variety of available inducible promoters that can be used in *Arabidopsis thaliana* and other model systems, both chemically induced by compounds

distinct from those used in mammalian systems (ethanol, dexamethasone, and β-estradiol) (Borghi, 2010) as well as the promoter of the *Arabidopsis* heat-shock protein *HSP18.2* gene, which is a strong inducible promoter that is activated by heat shock (Matsuhara et al., 2000; Takahashi and Komeda, 1989).

Genetic studies in bacterial models have also been facilitated by the varied options of inducible promoters throughout the years. The study of the dynamics and function of cytoskeletal proteins like the MreCD complex (Leaver and Errington, 2005) in *Bacillus subtilis* relied on combining strains that allowed the depletion of the cell division protein FtsZ with the Plac promoter while titering the expression of proteins of the MreCD complex under Pxyl. Cell division protein complex assembly studies (Daniel et al., 1998; Marston and Errington, 1999) have also benefited from the use of multiple inducible promoters in the same cell - the function of the cell division protein FtsW, hypothesized to stabilize the cytokinetic ring in *Escherichia coli*, was proven to be distinct from that: FtsW recruits the transpeptidase FtsI to the cytoplasmic ring. The study of the FtsW function relied on depletion and repletion experiments under the control of the Pbad promoter, while inducing expression of other cell division proteins using the Plac promoter (Mercer and Weiss, 2002).

The use of inducible promoters in depletion and repletion experiments enhanced our understanding of essential genes by allowing the observation of emergent phenotypes before cell death. Furthermore, the development of degrons, like the ClpXP-based systems (Chowdhury et al., 2010; Griffith and Grossman, 2008; Lessner et al., 2007) was accomplished by using two different promoters, Pxyl and Pspank to express GFP and ComA with different degradation tags, allowing the authors to show that the ClpXP system can be used to differentially degrade two different proteins in the same cell. This system promoted the discovery of uncoupled transcriptional and translational mechanisms controlling cell cycle progression (Jadhav et al., 2022).

As *Haloferax volcanii* emerges as the most studied archaeal model due to its relative ease of cultivation and established genetics (Pohlschroder and Schulze, 2019), the development of molecular biology tools that allow the expression of multiple genes simultaneously becomes essential. Currently, the only inducible promoter available is the PtnaA promoter, which is induced by tryptophan (Large et al., 2007). The absence of other inducible promoters in *Haloferax* has been a bottleneck in recent studies. For example, experiments suggested during the review process stage for the work by Nußbaum and coworkers (Nußbaum et al., 2021) - which would indicate the hierarchy of recruitment of SepF by FtsZ1 or FtsZ2 - were not feasible due to a lack of a second inducible promoter in *H. volcanii*. To address this need in the *Haloferax* community, we have characterized two versions of the same promoter region: a strong constitutive and a new xylose-inducible promoter to be used as a tool for genetic studies in *H. volcanii*.

Methods

***Haloferax volcanii* cultures.** Cells were grown in 16x25 mm glass tubes with 3 ml of Hv-Cab (de Silva et al., 2020) at 42 ºC under constant agitation with the inducers D-xylose (Thermo Scientific Chemicals), L-arabinose (Thermo Scientific Chemicals), IPTG (Fisher Bioreagents), D-maltose (Fisher Bioreagents), or L-tryptophan (Thermo Scientific Chemicals) in the concentrations indicated.

Cloning and transformations. The eTR8 vector was constructed by Gibson assembly (Gibson et al., 2009) from two PCR fragments using the oligos oTR26 and oTR27 (msfGFP) and a linearized pTA962 digested with NdeI.

The eAD08 vector was constructed by Gibson assembly from two PCR fragments using the oligos oBL340 and oJM96 (to amplify the msfGFP fragment) and the linearized pTA962 digested with NcoI.

The pAL250::msfGFP and pAL750::msfGFP vectors were constructed by Gibson assembly from three PCR fragments using the oligos oBL169 and oBL345 (msfGFP, eTR8 as a template), oBL343 and oBL344 (the first 250 bp upstream to the HVO_B0027 start codon using the H. volcanii strain DS2 gDNA as a template) or oBL343 and oBL345 (the first 750 bp upstream to the HVO_B0027 start codon using the H. volcanii strain DS2 gDNA as a template), and a linearized pTA962 previously digested with KpnI and BamHI.

The pAL750 vector was created by Gibson assembly from three PCR fragments using the pAL::msfGFP vector as a template and the oligos oZC23 and oTR150 (pHV2 ori), oTR151 and oSB33 (pyrE2-Pxyl750 region), and oBL97 and oBL105 (E. coli oriC and AmpR cassette).

The pAL750::ftsZ1 and pAL750::ftsZ2 vectors were cloned by Gibson assembly of two fragments using the oligos oTR151 and oTR152 (ftsZ1) or oTR153 and oTR154 (ftsZ2) using the H. volcanii strain DS2 gDNA as a template, and a linear fragment of the pAL vector digested with NdeI.

All Gibson reactions were transformed into competent E. coli DH5α cells and clones confirmed by whole-plasmid sequencing (Plasmidsaurus). Plasmid preps were then transformed into *H. volcanii* using the method previously described (Dyall-Smith M., 2009), with 0.5 M EDTA (Thermo Scientific Catalog #J15694-AE) and PEG600 (Sigma, catalog # 87333-250G-F).

Growth curves. Cells were grown to an OD_{600} of ~0.5 and diluted to an OD_{600} of 0.05. Then, 200 µL of culture was placed in a 96-well flat-bottom plate (Corning Inc.). All wells surrounding the plate's edge (A and H rows, 1 and 12 columns) were filled with 200 µl of water to prevent media evaporation. Growth curves of three biological triplicates were performed using an EPOCH 2 microplate spectrophotometer (Agilent) with constant orbital shaking at 42 ºC. Data points were collected every 30 minutes.

Microscopy and Image Analysis. Cells were grown in Hv-Cab to mid-exponential OD_{600} without or with inducers as indicated. Cultures were then, concentrated 10-fold by centrifuging (3000xg for 2-5 minutes) and a 3 µL droplet of culture was placed on a 60x24 mm coverslip and gently covered with a 1.5x1.5 cm 0.25% Hv-cab agarose pad (SeaKem LE Agarose, Lonza). Staining with Ethidium Bromide (Invitrogen, catalog #15585-011) was performed by adding 3 µg/ml of the dye into the cell culture and incubating at 42 ºC for 5 minutes. Cells were then imaged at 42 ºC using a Nikon TI-2 Nikon Inverted Microscope within an Okolab H201 enclosure. Phase-contrast and GFP-fluorescence images were acquired with a Hamamatsu ORCA Flash 4.0 v3 sCMOS Camera (6.5 µm/pixel), CFI PlanApo Lambda 100x DM Ph3 Objective, and a Lumencor Sola II Fluorescent LED (380-760 nm). Image analysis was performed using FIJI (Schindelin et al., 2012). Cells were segmented by using the rolling ball background subtraction (value=20) on phase-contrast images, followed by thresholding (default) and using the analyze particles function with a minimum particle size of 0.2 μm^2. The mask was then used to acquire shape descriptor data and applied to the GFP channel (after background subtraction) for fluorescence quantification.

RNA extraction and sequencing. Every step was performed at room temperature unless otherwise indicated. Cells were grown to an OD_{600} of ~0.5 in xylose (10 mM), arabinose (10 mM), IPTG (1 mM), and maltose (1 mM) and harvested by centrifugation (4500xg for 10 minutes). RNA extraction was performed using 1 mL of TriZol (Invitrogen) per sample, followed by vigorous pipetting to lyse all cells in the sample. 200 µL of chloroform was then added to the sample mixture and samples were vortexed for 90 seconds. Samples were then centrifuged at 12,000xg at 4 ºC for 15 minutes, and the supernatant was collected and mixed with 2 µL of glycogen (Sigma Aldrich) and 400 µL of isopropanol (Thermo Scientific Chemicals). Samples were incubated overnight at -20 ºC. Samples were then centrifuged at 21,000xg, 4 ºC for 30 minutes and washed twice with 75% ethanol (Zaffagni et al., 2022). Samples were then treated with DNAse I (NEB) for 12 minutes at 37 ºC, followed by a second ethanol precipitation. Purified RNA was sent to SeqCenter for ribosome depletion using *Haloferax*-specific probes (Table S1) and sequencing. Results were mapped to the *H. volcanii* DS2 genome and analyzed using Geneious 2002.2. Transcripts per million separated by ORF and inducer can be found in Table S2. Raw sequencing data (.fastq files and quality control files) is available in Supplemental Materials.

Table 1: Plasmids used in this work

Alias	Plasmid	Reference
pTA962	pTA962	(Allers et al., 2010)
eAD8	pTA962::PfdX-msfGFP	This work
eTR8	pTA962::msfGFP	This work
eTR34	pAL750::msfGFP	This work
eTR36	pAL750	This work
eTR34	pAL750::msfGFP	This work
eTR38	pAL750::*ftsZ1*	This work
eTR40	pAL750::*ftsZ2*	This work
eBL82	pTA962::*ftsZ1*	This work
eBL86	pTA962::*ftsZ2*	This work
eBL227	pAL250::msfGFP	This work

Table 2: *Haloferax volcanii* strains used in this work

Alias	Genotype	Reference
DS2	wild-type	(Hartman et al., 2010)
H26	Δ*pyrE2*	(Allers et al., 2004)

aAD9	pTA962::PfdX-msfGFP	This work
aBL296	Δ*pyrE2* pAL250::msfGFP	This work
aTR24	Δ*pyrE2* pTA962::msfGFP	This work
aTR94	Δ*pyrE2* pAL750::msfGFP	This work
aTR102	Δ*pyrE2* pAL750	This work
aTR103	Δ*pyrE2* pAL750::ftsZ1	This work
aTR104	Δ*pyrE2* pAL750::ftsZ2	This work
aTR105	Δ*pyrE2* pTA962::ftsZ1	This work
aTR106	Δ*pyrE2* pTA962::ftsZ2	This work

Table 3: Oligos used in this work

Alias	Sequence (5'→3')
oBL97	AGGTGGCACTTTTCGG
oBL105	TGAGCAAAAGGCCAGC
oBL169	ATGCGAAAAGGGGAAGAATTGTTTAC
oBL340	GTGCTGCGTTCGCCATCTAGATCATTT-GTAAAGTTCATCCATTCCAT
oBL343	CTATAGGGCGAATTGGG-TACACCCGCCGACTCGGCGT
oBL344	AATTCTTCCCCTTTTCGCATTGCAG-TATCCTCATTACCAGC
oBL345	GCTCTAGAACTAGTGGATCCTCATTT-GTAAAGTTCATCCATTCCATGC
oBL365	ACGCCGAGTCGGCGGGTCCGGTAC-CGGGTCGA
oJM96	CCGAACTCTGCAGCCATGCGAAAAGGGGAA-GAATT
oSB33	GCACATTTCCCCGAA
oTR26	TTCGCGGACCTATTGCGCAT-ATGCGAAAAGGGGAAGAATTGTTTA
oTR27	ATCAAGCTTATCGATTTCATTCATTT-GTAAAGTTCATCCATTCC
oTR150	GGATACTGCATATGAGGATCCACTAGTT
oTR151	TGCAGTATCCTCATTACC
oTR152	AGAACTAGTGGATCCTCATACTACTCGAC-GTAGTCGATGTCTT
oTR153	GCTGGTAATGAGGATACTGCAATGGACTC-TATCGTCGGC
oTR154	TCTAGAACTAGTGGATCCTCATTTACCG-GATGACGT
oTR155	GGTAATGAGGATACTGCATATGCAGGA-TATCGTTCG
oZC23	GCTGGCCTTTTGCTCACATGAGCTTCTTTGAT-TCGAGC

Results

RNA-seq screening to identify new sugar-responsive promoters

To find native inducible promoters, we investigated four different sugars frequently used as inducers in other microbial models: arabinose (Guzman et al., 1995), xylose (Kim et al., 1996), maltose (Ming-Ming et al., 2006), and IPTG (Dubendorff and Studier, 1991). To determine the highest sugar concentrations we could use in *H. volcanii* cultures without compromising growth rates, cell size, and morphology, we titrated each sugar from 1 mM to 100 mM. Based on concentrations used to induce promoters in bacteria, we expected that concentrations higher than 1 mM could yield slow-growing, smaller cells. Surprisingly, we could only observe this outcome from cultures above 10 mM (Fig. 1A-B). Therefore, we followed focusing on concentrations at 10 mM.

Next, to map candidates for new inducible promoters, we employed RNA-seq from mid-exponential cultures with or without each of the four inducers. Using a set of specific probes for *H. volcanii* (Supplementary Table 1) (Pastor et al., 2022), we obtained a ribosomal RNA depletion of 99.7%, from a total number of reads of 120,234,156. By comparing the relative fold change of transcripts per million scale, we obtained 58 genes from which mRNA levels were significantly upregulated (log2 fold change ≥ 1 and p-value ≤ 0.05) for xylose, 42 by maltose, 0 for IPTG, and 45 for arabinose. We identified 15 downregulated genes (log2 fold change ≤ -1 and p-value ≤ 0.05) for xylose, 44 for maltose, 2 for IPTG, and 10 for arabinose (Supplemental table 2).

To create a shortlist of promoter candidates we could further validate experimentally, we arbitrarily selected genes above 5-fold or higher ratio change upon the addition of the inducer (Fig. 1C). Above this threshold, there were only 3 promoters, all of them mapped in the pHV3 chromosome regulating genes *HVO_B0027*, *HVO_B0034* and *HVO_B0232* (Fig. 1D). In all cases, the expression of candidate genes was upregulated upon addition of xylose or arabinose (regions 1 and 2). Nevertheless, we did not observe any maltose- or IPTG-induced genes which satisfied our stringent criteria (Supplemental table 2). However,

further inspection of the transcriptional profiles, we observed upregulated genes (Fig. 1C). Interestingly, whereas the genomic region comprising genes *HVO_B106* did not pass our requirements, it called our attention for being arabinose-specific and not being significantly upregulated under xylose addition (Fig 1C, orange arrowhead). Likewise, genes *HVO_0562-HVO_0566* are specifically upregulated under maltose induction (Fig. 1C, green arrowhead), and three regions (*HVO_A0173*, *HVO_B0032*, and *HVO_B0303*) respond to IPTG (Fig 1C, pink arrowheads).

dataset in the uninduced sample (1.44 TPM and 23.65 TPM, respectively).

Altogether, either genomic regions 1 and 2 are promising candidates for new xylose- and arabinose-inducible promoters for *H. volcanii*. For the context of this work, and based on the dynamic range suggested by our RNA-seq dataset above, we focused on the characterization of the promoter regulating the gene *xacE* (*HVO_B0027*) under the induction of xylose.

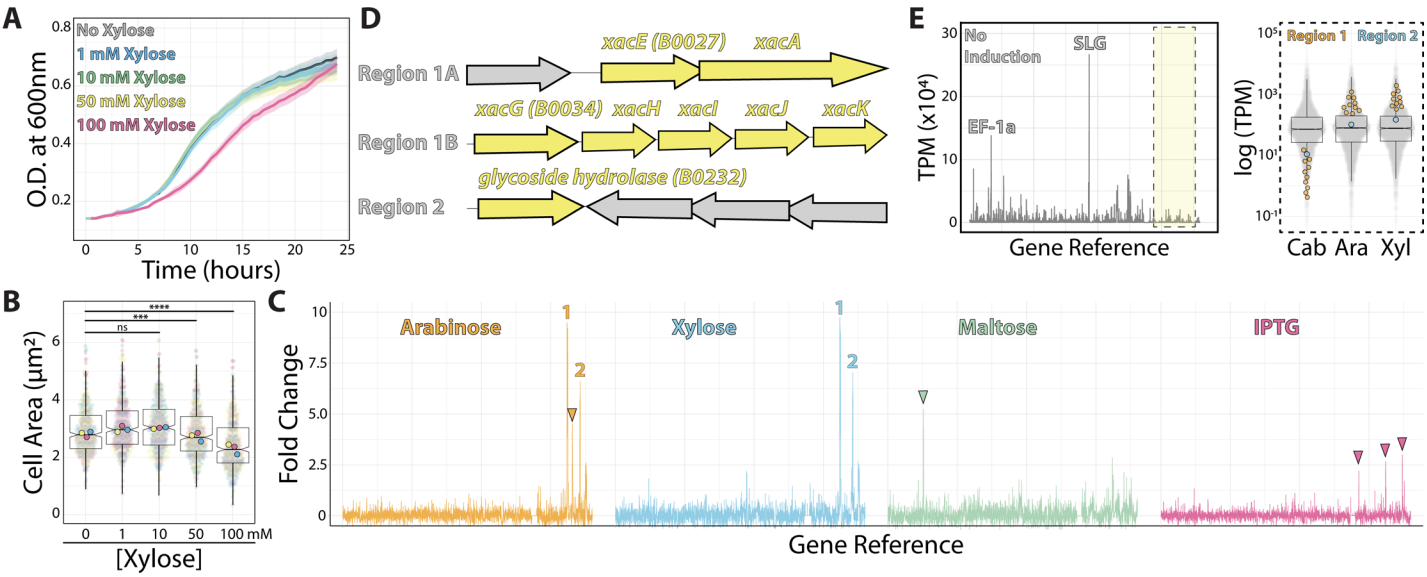

Figure 1: RNA-seq map of inducer-responsive promoters in H. volcanii. (A) growth curves of *H. volcanii* DS2 cells under different xylose concentrations. (B) Cell area measurements at different xylose concentrations by phase contrast microscopy from mid-exponential cultures. (C) Gene expression ratios mapped across the *H. volcanii* genome from RNA-seq datasets of mid-exponential cultures with and without 10 mM arabinose (orange), xylose (blue), maltose (green), and IPTG (pink). Numbers 1 and 2 indicate genomic regions where gene expression increased above 5-fold. Arrowheads indicate promising genomic regions that did not satisfy our arbitrary 5-fold cutoff. (D) locus organization of regions 1 and 2. (E) Expression map (transcripts per million) of genomic regions from RNA-seq datasets without inducers (left) and the relative increase in expression (right) from uninduced (Cab) and arabinose (Ara) and xylose (Xyl).

Despite observing an approximately 10-fold increase in mRNA levels upon inducer addition, we wanted to make sure these genes were not already constitutively expressed at a high basal expression level. This becomes important if we aim to have a tightly controlled inducible promoter with precise linear titration power. To understand the basal expression levels of genes including regions 1 and 2, we plotted the raw transcription profile (Fig 1E, left panel) and compared it to the transcriptional levels of all other genes (Fig 1E, right panel). As expected, after ribosomal RNA depletion, the transcripts with higher relative values in our datasets were the ones mapping to the S-layer glycoprotein (csg, over 26,000 TPM across samples) and the translational factor EF1a transcripts (above 10,000 TPM across samples). On the other hand, both promoter regions 1 and 2 transcriptional levels are placed in the low quartile range of our

The *xacEA* 5' untranslated region is required for *xacE* repression in the absence of xylose

To put the *xacE* promoter region to test, we sub-cloned the fluorescent protein msfGFP under the control of two different putative promoter regions: 250 bp (P250) and 750 bp (P750) upstream to *xacE* (Fig. 2A). Plasmids were then transformed into *H. volcanii* H26 (Δ*pyrE2*), a strain incapable of producing uracil without the *pyrE2* gene (Allers et al., 2004), and selected on plates without uracil. As a negative control, we used the H26 strain transformed with the empty pAL750 vector (labeled from now on as wild type). As a comparison, we also used an identical construct, but having msfGFP under the control of the popular inducible promoter PtnaA, which activates upon tryptophan addition (Allers et al., 2010). As a benchmark, we also inserted msfGFP under the control of PfdX, a strong and constitutive promoter used

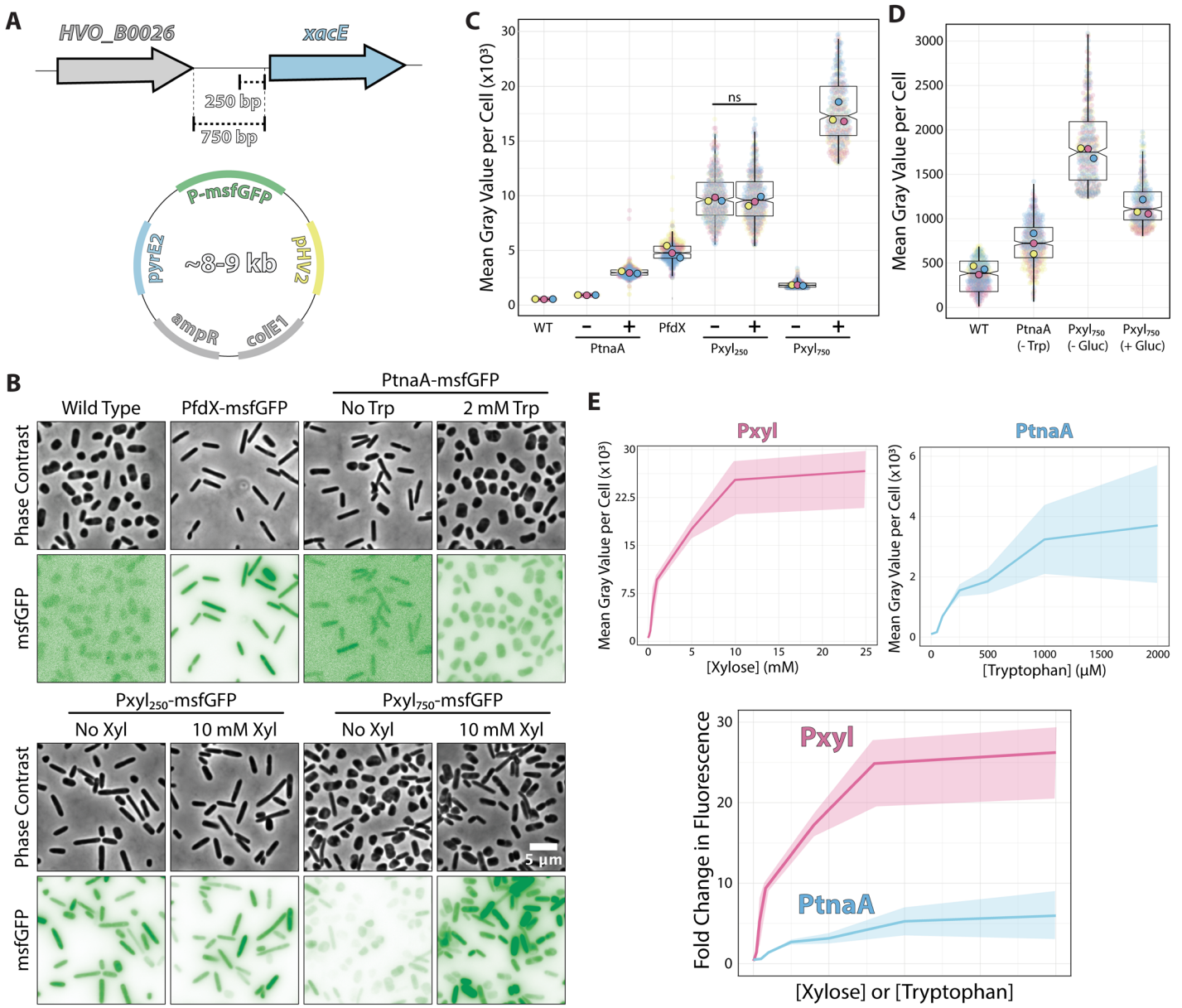

Figure 2: Pxyl constructs can be either strong inducible or constitutive promoters. (A) Fragments of the 5' intergenic region of *xacE* were used to clone into pAL vectors and map the P250 and P750 promoters tested in this work. (B) Phase-contrast and epifluorescence images of different constructs expressing the msfGFP fluorescent protein. (C) Mean msfGFP fluorescence measurements per cell from images shown in panel B. Each replicate mean and data points are independently labeled with different colors (pink, yellow and blue) (D) Comparative background expression from constructs with and without glucose repression. (E) The dynamic range of PtnaA and Pxyl promoters across different inducer concentrations in raw numbers (top) and normalized (bottom) fold-changes. Shades indicate the 95% confidence interval from triplicate datasets.

to express the *pyrE2* gene in our vectors as a selective transformation marker (*PfdX-msfGFP-pyrE2* operon).

Imaging live cells by phase-contrast and epifluorescence microscopy, we observed the cytoplasmic signal emitted by the msfGFP fluorescent protein from single cells (Fig. 2B). Cells carrying empty plasmids (Fig. 2B, first column) showed low auto-fluorescence at 488 nm excitation compared to cells carrying vectors inducing msfGFP under the control of PfdX and Pxyl promoters. For a quantitative picture of the induction power of each promoter, we segmented individual cells and measured the mean fluorescence per cell from three biological triplicates and graphed using SuperPlots (Goedhart, 2021; Lord et al., 2020). Surprisingly, the P250 promoter was not only insensitive to xylose but also constitutively expressed 2-fold above the PfdX

control (10,048±2,256 and 4,967±929, respectively) (Fig. 2C).

In contrast, the P750 promoter harboring the whole 5' UTR sequence showed approximately a 5.5-fold repression (1,827±848) without induction in comparison to P250. However, msfGFP levels of non-induced P750 cells were still relatively high, only 1.7-fold lower in comparison to PtnaA cells under the induction with 2 mM tryptophan (3160±529) (Fig. 2B and C). To minimize the transcriptional leakage from P750, we tested whether Haloferax cells would present catabolite repression upon the addition of glucose. This strategy has been shown successfully in a variety of bacterial and yeast systems (Deutscher, 2008; Gancedo, 1998). The addition of 20 mM glucose to cultures decreased leakage of msfGFP 1.6-fold (Fig. 2D), but still 2.1-fold higher than PtnaA cells.

However, different from the P250 promoter, the addition of 10 mM xylose to P750 cells resulted in a 10.3-fold increase (18792±4129) in fluorescence emission with a wider heterogeneity across the population compared to P250. Nevertheless, the unusual decrease in msfGFP expression observed between P250 and P750 suggests the 5' region of xacE may be regulated either at the promoter or mRNA levels.

Finally, we inspected the dynamic range of our P750 promoter compared to PtnaA. By titrating xylose (0 to 25 µM) and tryptophan (0 to 2 mM), we observed a significant improvement from an 11.2-fold linear range for the PtnaA to a 23-fold for the P750 promoter (Fig. 2E). Providing the relatively higher leakage of the P750 promoter levels compared to PtnaA, we concluded that this new construct is ideal for titration experiments and overexpression at high protein levels for functional studies in *H. volcanii*. Notably, P250 can be used simultaneously with the above inducible promoters as yet another constitutive promoter in the Haloferax community.

Overexpression of the tubulins FtsZ1 and FtsZ2 confirms reported morphological phenotypes

Recently, Liao and colleagues reported the role of two tubulin paralogs (FtsZ1 and FtsZ2) in *H. volcanii*'s cell division (Liao et al., 2021). The authors used PtnaA-controlled overexpression of FtsZ1 and FtsZ2 independently and observed distinct, specific morphological phenotypes related to each paralog. Cells under PtnaA-FtsZ1 overexpression were slightly larger but significantly misshaped compared to the control, whereas PtnaA-FtsZ2 cells looked significantly smaller but showed a more consistent morphology.

To confirm if those phenotypes are reproducible or even enhanced in our new Pxyl system, we cloned ftsZ1 and ftsZ2 in the pAL vector and analyzed the cell size and circularity in comparison to PtnaA-induced cells. Cells overexpressing ftsZ2 under the Pxyl promoter are slightly smaller (1.2-fold decrease in average cell area) than cells overexpressing ftsZ2 under the tryptophan-inducible PtnaA (Fig 4A and C). Meanwhile, cells overexpressing ftsZ1 under the Pxyl promoter seemed to have more drastic phenotypes than those overexpressing ftsZ1 using PtnaA (Fig. 4A), with deformed and enlarged cells (Fig 4A and C). Curiously, a fraction of the population exhibits narrow "cell bridges" connecting two enlarged cells (Fig. 4B), similar to those previously described (Rosenshine et al., 1989; Sivabalasarma et al., 2021; von Kügelgen et al., 2021). When DNA in cells was stained with ethidium bromide, we observed a homogeneous signal across the cell-to-cell bridges. This indicates that the cell-to-cell bridges observed in phase contrast are formed by two communicating cells, instead of clumps. We hypothesize that the cell bridges observed here are a product of incomplete cell division.

Discussion

Inducible promoters have been an invaluable resource in molecular biology basic research for the past 60 years, since the early days of the "PaJaMa Experiments" (Lewis, 2011). The addition of xylose to the culture medium was first shown to induce the expression of genes in *E. coli* (Batt et al., 1985) and *B. subtilis* in 1988 (Gärtner et al., 1988). The cloning of xylose-induced promoters in an inducible expression system was first described in *Staphylococcus carnosus* in 1995 (Wieland et al., 1995) and in *B. subtillis* in 1996 (Kim et al., 1996). Since then, in eukaryotes, xylose-inducible promoters have been described in various fungal species (Yap et al., 2022) and adapted and optimized for *S. cerevisiae* (Hector et al., 2019). In bacteria, the Pxyl promoter has been extensively used in Caulobacter crescentus (Stephens et al., 2007) and more recently for *Streptomyces* (Noguchi et al., 2018), *Pseudomonas* (Callaghan et al., 2020), and *Clostridioides difficile* (Müh et al., 2019). Finally, in 2020, a xylose-inducible promoter was first cloned and used to express heterologous proteins in the thermoacidophilic archaeon *Sulfolobus acidocaldarius* (van der Kolk et al., 2020). In this succinct report, we describe the characterization of a new xylose-inducible promoter for the halophilic archaeon *H. volcanii*, the most studied archaeal model (Pohlschroder and Schulze, 2019).

Using RNA-seq in cultures growing with and without four different inducers, we identified multiple genomic regions in which transcript levels were upregulated upon the addition of arabinose (3 gene clusters), xylose (2 gene clusters), maltose (1 gene cluster) and IPTG (3 gene clusters). Interestingly, our most promising promoter chosen to be characterized was already noted in past studies using DNA microarrays and C13 isotope tracking (Johnsen et al., 2009) and further characterized in vitro and in vivo (Johnsen et al., 2015, 2013). However, their measurements (ranging from 100- to 400-fold increase upon arabinose addition) were greatly overestimated compared to our observations from our RNA-seq (9.8-fold, Fig. 1C) and live-cell microscopy (10.3-fold increase, Fig. 2C). Curiously, against the anecdotal knowledge among researchers in the field, PtnaA-msfGFP showed a relatively low leakage in cultures without tryptophan (Fig. 2D). However, it is possible that the reported leakage issues with PtnaA are not originated from transcriptional activation, but from the stability of each specific protein.

One interesting previously unmentioned feature of the transcriptional regulation of the *xacEA* operon is that the P750 promoter not only is significantly repressed in the absence of xylose, but P750 shows a 1.9-fold increase in msfGFP signal in comparison to the constitutive P250 promoter (Fig. 2C). The mechanistic details are still elusive, but it is possible that the extreme 5' UTR is the target of transcriptional factors competing to repress and activate the expression of xacEA. A good candidate for activator is XacR (HVO_B0040), an IclR transcriptional factor family shown to moonlight between repression and activation (Krell et al., 2006; Pan et al., 2011). In agreement with previous observations in bacteria, XacR in H. volcanii was shown to be required for activation of *xacE* expression in vivo (Johnsen et al., 2015).

To put our Pxyl promoter to a test, we have shown that, through the use of higher levels of expression than with the available promoter PtnaA, cells overexpressing the tubulin-like FtsZ1 resulted in drastic cell morphology defects (Fig. 3) beyond the previously described (Liao et al., 2021). Interestingly, FtsZ2 overexpressing under our Pxyl system did not result in a convincing difference to PtnaA-ftsZ2 cells, in agreement with data suggesting FtsZ2 proteins are more unstable compared to FtsZ1 (Liao et al., 2021). Hence, Pxyl-based overexpression experiments can be especially fruitful for protein complexes with longer lifetimes.

Aside from the Pxyl promoter, we mapped other promoter regions that showed to be independently upregulated upon the addition of maltose and IPTG (Fig. 1C). The characterization of these promoters may expand the toolbox of inducible promoters in *H. volcanii* in the future.

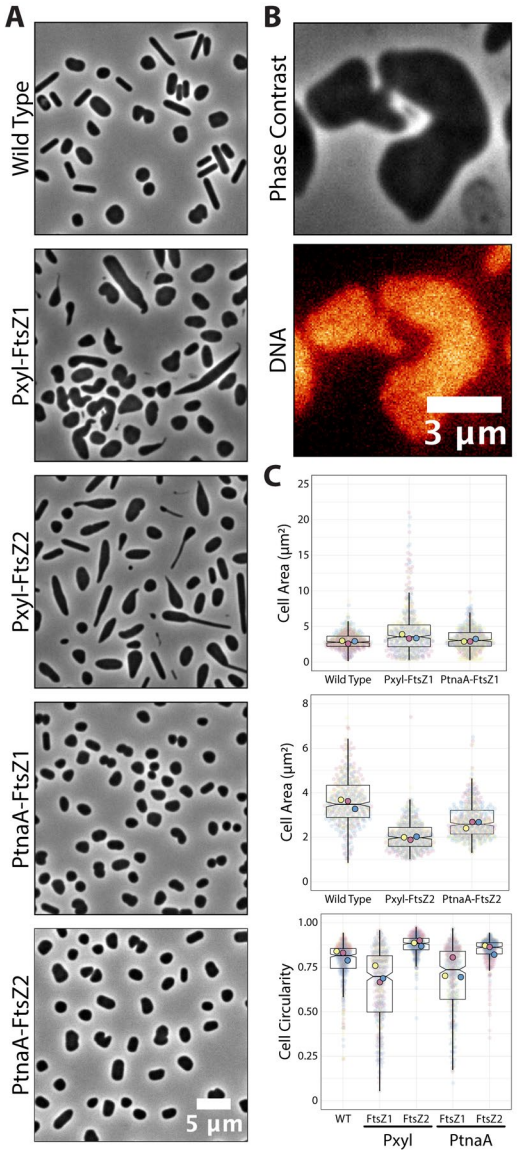

Figure 3: Overexpression of ftsZ1 and ftsZ2 under the Pxyl promoter. (A) Phase-contrast microscopy showing wild-type, overexpressing ftsZ1 or ftsZ2 cells under the Pxyl (5 mM xylose) or PtnaA (2 mM tryptophan) promoters. (B) Representative cell bridge phase-contrast and epifluorescence images. DNA was stained with ethidium bromide. (C) Cell area and circularity measurements from cells overexpressing ftsZ1 and ftsZ2 with the Pxyl (5 mM xylose) and the PtnaA (2 mM tryptophan) promoters. Each replicate mean and data points are independently labeled with different colors (pink, yellow and blue).

Data Availability

The complete raw RNA-seq datasets presented in this study can be found in online repositories: PRJNA953041 (no

induction) PRJNA953037 (xylose) PRJNA953035 (IPTG) PRJNA953033 (Arabinose), PRJNA953034 (Maltose).

Acknowledgments

We thank the Bisson Lab, Kiwi Shaw-Dodge and Rosana De Castro (Universidad Nacional de Mar del Plata, Mar del Plata) for insightful comments on our manuscript. We appreciate Sebastian Kadener and Sinead Nguyen (Brandeis University) for their help in optimizing the total RNA extraction from *H. volcanii* cultures. We are also grateful to Amy Schmid and Mar Martinez-Pastor (Duke University) for sharing data ahead of publication on their ribodepletion probes. This work was supported by the Human Frontiers Science Program funding (RGY0074/2021) and Life Sciences-Moore–Simons Project on the Origin of the Eukaryotic Cell (https://doi.org/10.46714/735929LPI) awarded to AB. AB is a Pew Scholar in the Biomedical Sciences, supported by The Pew Charitable Trusts. MC was supported by the CONICET Partial Financing Program for Stays Abroad for Assistant Researchers.

Author Contributions

AB and TR conceived the study. AB, MC, TR, and KA designed the experiments. TR and KA performed the experiments and analyzed the data. AB and TR wrote the first draft. All authors reviewed and approved the submitted version.

Conflict of Interest

The authors declare that the research was conducted in the absence of any commercial or financial relationships that could be construed as a potential conflict of interest.

References

Allers, T., Barak, S., Liddell, S., Wardell, K., Mevarech, M., 2010. Improved strains and plasmid vectors for conditional overexpression of His-tagged proteins in Haloferax volcanii. Appl. Environ. Microbiol. 76, 1759–69. https://doi.org/10.1128/AEM.02670-09

Allers, T., Ngo, H.-P., Mevarech, M., Lloyd, R.G., 2004. Development of additional selectable markers for the halophilic archaeon Haloferax volcanii based on the leuB and trpA genes. Appl. Environ. Microbiol. 70, 943–53. https://doi.org/10.1128/aem.70.2.943-953.2004

Batt, C.A., Bodis, M.S., Picataggio, S.K., Claps, M.C., Jamas, S., Sinskey, A.J., 1985. Analysis of xylose operon regulation by Mud (Apr, lac) fusion: trans effect of plasmid coded xylose operon. Can. J. Microbiol. 31, 930–933. https://doi.org/10.1139/m85-174

Borghi, L., 2010. Inducible Gene Expression Systems for Plants, in: Hennig, L., Köhler, C. (Eds.), Plant Developmental Biology: Methods and Protocols, Methods in Molecular Biology. Humana Press, Totowa, NJ, pp. 65–75. https://doi.org/10.1007/978-1-60761-765-5_5

Callaghan, J.D., Stella, N.A., Lehner, K.M., Treat, B.R., Brothers, K.M., St Leger, A.J., Shanks, R.M.Q., 2020. Xylose-Inducible Promoter Tools for Pseudomonas Species and Their Use in Implicating a Role for the Type II Secretion System Protein XcpQ in the Inhibition of Corneal Epithelial Wound Closure. Appl. Environ. Microbiol. 86, e00250-20. https://doi.org/10.1128/AEM.00250-20

Chowdhury, T., Chien, P., Ebrahim, S., Sauer, R.T., Baker, T.A., 2010. Versatile modes of peptide recognition by the ClpX N domain mediate alternative adaptor-binding specificities in different bacterial species. Protein Sci. Publ. Protein Soc. 19, 242–254. https://doi.org/10.1002/pro.306

Daniel, R.A., Harry, E.J., Katis, V.L., Wake, R.G., Errington, J., 1998. Characterization of the essential cell division gene ftsL (yllD) of Bacillus subtilis and its role in the assembly of the division apparatus. Mol. Microbiol. 29, 593–604. https://doi.org/10.1046/j.1365-2958.1998.00954.x

de Silva, R.T., Abdul-Halim, M.F., Pittrich, D.A., Brown, H.J., Pohlschroder, M., Duggin, I.G., 2021. Improved growth and morphological plasticity of Haloferax volcanii. Microbiology 167, 001012. https://doi.org/10.1099/mic.0.001012

Deutscher, J., 2008. The mechanisms of carbon catabolite repression in bacteria. Curr. Opin. Microbiol. 11, 87–93. https://doi.org/10.1016/j.mib.2008.02.007

Dubendorff, J.W., Studier, F.W., 1991. Controlling basal expression in an inducible T7 expression system by blocking the target T7 promoter with lac repressor. J. Mol. Biol. 219, 45–59. https://doi.org/10.1016/0022-2836(91)90856-2

Dyall-Smith M., 2009. The Halohandbook: Protocols for Halobacterial Genetics Ver 7.2.

Gancedo, J.M., 1998. Yeast Carbon Catabolite Repression. Microbiol. Mol. Biol. Rev. 62, 334–361.

Gärtner, D., Geissendörfer, M., Hillen, W., 1988. Expression of the Bacillus subtilis xyl operon is repressed at the level of transcription and is induced by xylose. J. Bacteriol. 170, 3102–3109.

Gibson, D.G., Young, L., Chuang, R.-Y., Venter, J.C., Hutchison, C.A., Smith, H.O., 2009. Enzymatic assembly of DNA molecules up to several hundred kilobases. Nat. Methods 6, 343–5. https://doi.org/10.1038/nmeth.1318

Goedhart, J., 2021. SuperPlotsOfData—a web app for the transparent display and quantitative comparison of continuous data from different conditions. Mol. Biol. Cell 32, 470–474. https://doi.org/10.1091/mbc.E20-09-0583

Griffith, K.L., Grossman, A.D., 2008. Inducible protein degradation in Bacillus subtilis using heterologous peptide tags and adaptor proteins to target substrates to the protease ClpXP. Mol. Microbiol. 70, 1012–1025. https://doi.org/10.1111/j.1365-2958.2008.06467.x

Guzman, L.M., Belin, D., Carson, M.J., Beckwith, J., 1995. Tight regulation, modulation, and high-level expression by vectors containing the arabinose PBAD promoter. J. Bacteriol. 177, 4121–4130.

Hartman, A.L., Norais, C., Badger, J.H., Delmas, S., Haldenby, S., Madupu, R., Robinson, J., Khouri, H., Ren, Q., Lowe, T.M., Maupin-Furlow, J., Pohlschroder, M., Daniels, C.,

Pfeiffer, F., Allers, T., Eisen, J.A., 2010. The complete genome sequence of Haloferax volcanii DS2, a model archaeon. PloS One 5, e9605. https://doi.org/10.1371/journal.pone.0009605

Hector, R.E., Mertens, J.A., Nichols, N.N., 2019. Development and characterization of vectors for tunable expression of both xylose-regulated and constitutive gene expression in Saccharomyces yeasts. New Biotechnol. 53, 16–23. https://doi.org/10.1016/j.nbt.2019.06.006

Jadhav, P., Chen, Y., Butzin, N., Buceta, J., Urchueguía, A., 2022. Bacterial degrons in synthetic circuits. Open Biol. 12, 220180. https://doi.org/10.1098/rsob.220180

Johnsen, U., Dambeck, M., Zaiss, H., Fuhrer, T., Soppa, J., Sauer, U., Schönheit, P., 2009. d-Xylose Degradation Pathway in the Halophilic Archaeon Haloferax volcanii. J. Biol. Chem. 284, 27290–27303. https://doi.org/10.1074/jbc.M109.003814

Johnsen, U., Sutter, J.-M., Schulz, A.-C., Tästensen, J.-B., Schönheit, P., 2015. XacR – a novel transcriptional regulator of D-xylose and L-arabinose catabolism in the haloarchaeon Haloferax volcanii. Environ. Microbiol. 17, 1663–1676. https://doi.org/10.1111/1462-2920.12603

Johnsen, U., Sutter, J.-M., Zaiß, H., Schönheit, P., 2013. l-Arabinose degradation pathway in the haloarchaeon Haloferax volcanii involves a novel type of l-arabinose dehydrogenase. Extremophiles 17, 897–909. https://doi.org/10.1007/s00792-013-0572-2

Kallunki, T., Barisic, M., Jäättelä, M., Liu, B., 2019. How to Choose the Right Inducible Gene Expression System for Mammalian Studies? Cells 8, 796. https://doi.org/10.3390/cells8080796

Kim, L., Mogk, A., Schumann, W., 1996. A xylose-inducible Bacillus subtilis integration vector and its application. Gene 181, 71–76. https://doi.org/10.1016/s0378-1119(96)00466-0

Krell, T., Molina-Henares, A.J., Ramos, J.L., 2006. The IclR family of transcriptional activators and repressors can be defined by a single profile. Protein Sci. Publ. Protein Soc. 15, 1207–1213. https://doi.org/10.1110/ps.051857206

Large, A., Stamme, C., Lange, C., Duan, Z., Allers, T., Soppa, J., Lund, P.A., 2007. Characterization of a tightly controlled promoter of the halophilic archaeon Haloferax volcanii and its use in the analysis of the essential cct1 gene. Mol. Microbiol. 66, 1092–1106. https://doi.org/10.1111/j.1365-2958.2007.05980.x

Leaver, M., Errington, J., 2005. Roles for MreC and MreD proteins in helical growth of the cylindrical cell wall in Bacillus subtilis. Mol Microbiol 57, 1196–1209.

Lessner, F.H., Venters, B.J., Keiler, K.C., 2007. Proteolytic Adaptor for Transfer-Messenger RNA-Tagged Proteins from α-Proteobacteria. J. Bacteriol. 189, 272–275. https://doi.org/10.1128/JB.01387-06

Lewis, M., 2011. A tale of two repressors – a historical perspective. J. Mol. Biol. 409, 14–27. https://doi.org/10.1016/j.jmb.2011.02.023

Liao, Y., Ithurbide, S., Evenhuis, C., Löwe, J., Duggin, I.G., 2021. Cell division in the archaeon Haloferax volcanii relies on two FtsZ proteins with distinct functions in division ring assembly and constriction. Nat. Microbiol. 6, 594–605. https://doi.org/10.1038/s41564-021-00894-z

Lord, S.J., Velle, K.B., Mullins, R.D., Fritz-Laylin, L.K., 2020. SuperPlots: Communicating reproducibility and variability in cell biology. J. Cell Biol. 219, e202001064. https://doi.org/10.1083/jcb.202001064

Marston, A.L., Errington, J., 1999. Selection of the midcell division site in Bacillus subtilis through MinD-dependent polar localization and activation of MinC. Mol Microbiol 33, 84–96.

Matsuhara, S., Jingu, F., Takahashi, T., Komeda, Y., 2000. Heat-shock tagging: a simple method for expression and isolation of plant genome DNA flanked by T-DNA insertions. Plant J. 22, 79–86. https://doi.org/10.1046/j.1365-313x.2000.00716.x

Mercer, K.L., Weiss, D.S., 2002. The Escherichia coli cell division protein FtsW is required to recruit its cognate transpeptidase, FtsI (PBP3), to the division site. J Bacteriol 184, 904–12.

Ming-Ming, Y., Wei-Wei, Z., Xi-Feng, Z., Pei-Lin, C., 2006. Construction and characterization of a novel maltose inducible expression vector in Bacillus subtilis. Biotechnol. Lett. 28, 1713–1718. https://doi.org/10.1007/s10529-006-9146-z

Müh, U., Pannullo, A.G., Weiss, D.S., Ellermeier, C.D., 2019. A Xylose-Inducible Expression System and a CRISPR Interference Plasmid for Targeted Knockdown of Gene Expression in Clostridioides difficile. J. Bacteriol. 201, e00711-18. https://doi.org/10.1128/JB.00711-18

Noguchi, Y., Kashiwagi, N., Uzura, A., Ogino, C., Kondo, A., Ikeda, H., Sota, M., 2018. Development of a strictly regulated xylose-induced expression system in Streptomyces. Microb. Cell Factories 17, 151. https://doi.org/10.1186/s12934-018-0991-y

Nußbaum, P., Gerstner, M., Dingethal, M., Erb, C., Albers, S.-V., 2021. The archaeal protein SepF is essential for cell division in Haloferax volcanii. Nat. Commun. 12, 3469. https://doi.org/10.1038/s41467-021-23686-9

Pan, Y., Fiscus, V., Meng, W., Zheng, Z., Zhang, L.-H., Fuqua, C., Chen, L., 2011. The Agrobacterium tumefaciens Transcription Factor BlcR Is Regulated via Oligomerization. J. Biol. Chem. 286, 20431–20440. https://doi.org/10.1074/jbc.M110.196154

Pastor, M.M., Sakrikar, S., Rodriguez, D.N., Schmid, A.K., 2022. Comparative Analysis of rRNA Removal Methods for RNA-Seq Differential Expression in Halophilic Archaea. Biomolecules 12, 682. https://doi.org/10.3390/biom12050682

Pohlschroder, M., Schulze, S., 2019. Haloferax volcanii. Trends Microbiol. 27, 86–87. https://doi.org/10.1016/j.tim.2018.10.004

Rosenshine, I., Tchelet, R., Mevarech, M., 1989. The mechanism of DNA transfer in the mating system of an archaebacterium. Science 245, 1387–9.

Schindelin, J., Arganda-Carreras, I., Frise, E., Kaynig, V., Longair, M., Pietzsch, T., Preibisch, S., Rueden, C., Saalfeld, S., Schmid, B., Tinevez, J.-Y.J.-Y., White, D.J., Hartenstein, V., Eliceiri, K., Tomancak, P., Cardona, A., Liceiri, K., Tomancak, P., A., C., 2012. Fiji: an open source platform for biological image analysis. Nat. Methods 9, 676–682. https://doi.org/10.1038/nmeth.2019.Fiji

Sivabalasarma, S., Wetzel, H., Nußbaum, P., van der Does, C., Beeby, M., Albers, S.-V., 2021. Analysis of Cell–Cell Bridges in Haloferax volcanii Using Electron Cryo-Tomography Reveal a Continuous Cytoplasm and S-Layer. Front. Microbiol. 11.

Stephens, C., Christen, B., Watanabe, K., Fuchs, T., Jenal, U., 2007. Regulation of d-Xylose Metabolism in Caulobacter crescentus by a LacI-Type Repressor. J. Bacteriol. 189, 8828–8834. https://doi.org/10.1128/JB.01342-07

Takahashi, T., Komeda, Y., 1989. Characterization of two genes encoding small heat-shock proteins in Arabidopsis thaliana. Mol. Gen. Genet. MGG 219, 365–372. https://doi.org/10.1007/BF00259608

van der Kolk, N., Wagner, A., Wagner, M., Waßmer, B., Siebers, B., Albers, S.-V., 2020. Identification of XylR, the Activator of Arabinose/Xylose Inducible Regulon in Sulfolobus acidocaldarius and Its Application for Homologous Protein Expression. Front. Microbiol. 11, 1066. https://doi.org/10.3389/fmicb.2020.01066

von Kügelgen, A., Alva, V., Bharat, T.A.M., 2021. Complete atomic structure of a native archaeal cell surface. Cell Rep. 37, 110052. https://doi.org/10.1016/j.celrep.2021.110052

Weinhandl, K., Winkler, M., Glieder, A., Camattari, A., 2014. Carbon source dependent promoters in yeasts. Microb. Cell Factories 13, 5. https://doi.org/10.1186/1475-2859-13-5

Wieland, K.-P., Wieland, B., Götz, F., 1995. A promoter-screening plasmid and xylose-inducible, glucose-repressible expression vectors for Staphylococcus carnosus. Gene 158, 91–96. https://doi.org/10.1016/0378-1119(95)00137-U

Yap, A., Glarcher, I., Misslinger, M., Haas, H., 2022. Characterization and engineering of the xylose-inducible xylP promoter for use in mold fungal species. Metab. Eng. Commun. 15, e00214. https://doi.org/10.1016/j.mec.2022.e00214

Zaffagni, M., Harris, J.M., Patop, I.L., Pamudurti, N.R., Nguyen, S., Kadener, S., 2022. SARS-CoV-2 Nsp14 mediates the effects of viral infection on the host cell transcriptome. eLife 11, e71945. https://doi.org/10.7554/eLife.71945